ADVANCED ENERGY MATERIALS

Supporting Information

for *Adv. Energy Mater.*, DOI 10.1002/aenm.202304091

Stabilizing Multi-Electron NASICON-$Na_{1.5}V_{0.5}Nb_{1.5}(PO_4)_3$ Anode via Structural Modulation for Long-Life Sodium-Ion Batteries

*Biplab Patra, Rashmi Hegde, Anirudh Natarajan, Debolina Deb, Dorothy Sachdeva, Narayanan Ravishankar, Keshav Kumar, Gopalakrishnan Sai Gautam and Premkumar Senguttuvan**

WILEY-VCH

Supporting Information

Stabilizing Multi-electron NASICON-$Na_{1.5}V_{0.5}Nb_{1.5}(PO_4)_3$ Anode via Structural Modulation for Long-life Sodium-ion Batteries

Biplab Patra, Rashmi Hegde, Anirudh Natarajan, Debolina Deb, Dorothy Sachdeva, Narayanan Ravishankar, Keshav Kumar, Gopalakrishnan Sai Gautam, and Premkumar Senguttuvan *

B. Patra, R. Hegde, K. Kumar, P. Senguttuvan
New Chemistry Unit, International Centre for Materials Science, and School of Advanced Materials
Jawaharlal Nehru Centre for Advanced Scientific Research
Jakkur, Bangalore-560064, India.

A. Natarajan, D. Deb, G.S. Gautam
Department of Materials Engineering
Indian Institute of Science, Bengaluru-560012, India.

A. Natarajan
Department of Metallurgical and Materials Engineering,
National Institute of Technology, Tiruchirappalli- 620015, India.

D. Sachdeva, N. Ravishankar
Materials Research Centre
Indian Institute of Science, Bengaluru-560012, India.

Email: prem@jncasr.ac.in

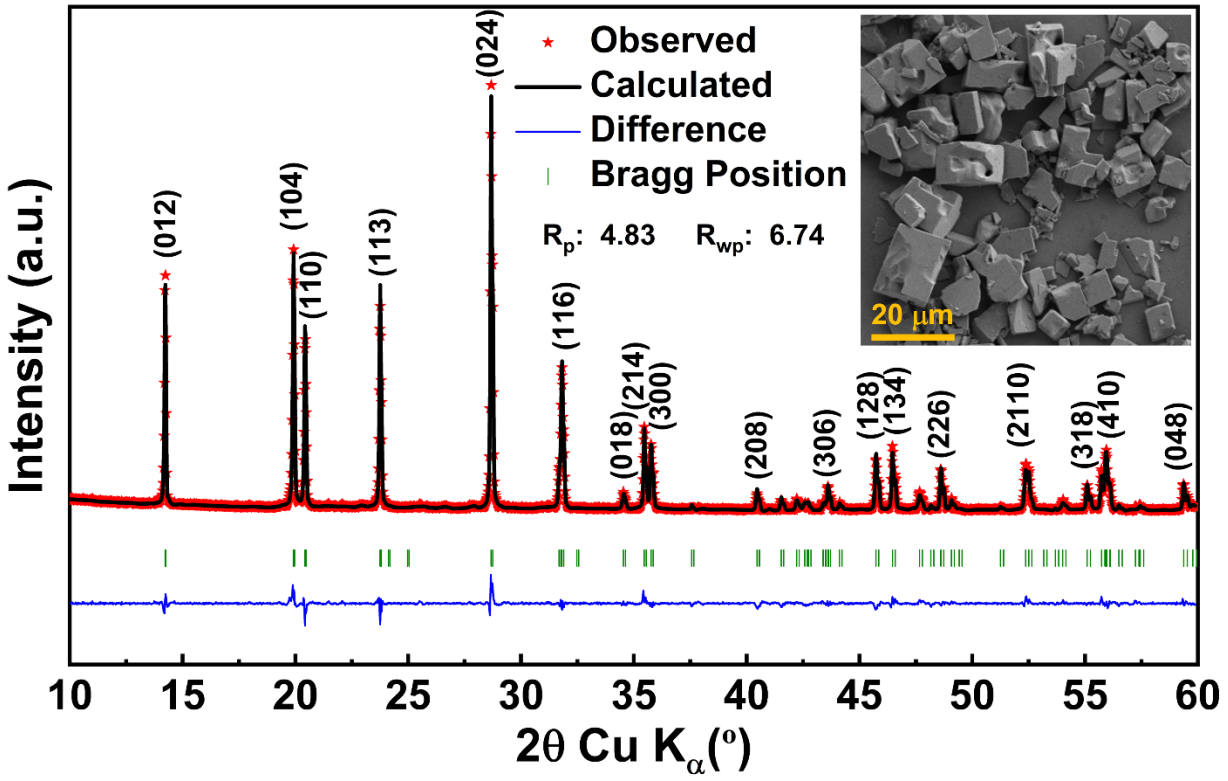

Figure S1. Rietveld refinement profile of the X-ray diffraction (XRD) pattern obtained for $Na_0Nb_2(PO_4)_3$ (N_0NbP). Inset shows scanning electron microscopy (SEM) image of N_0NbP.

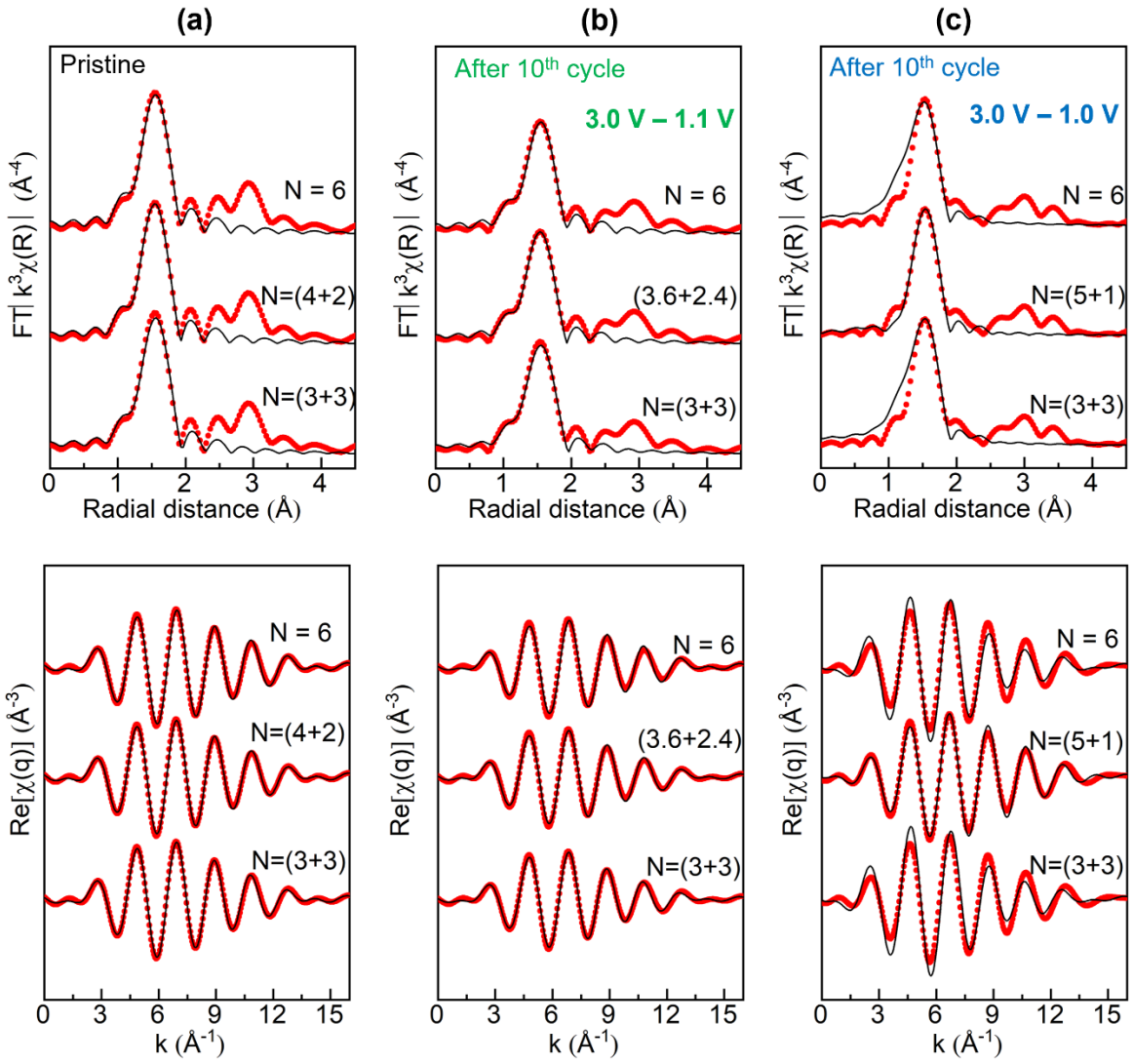

Figure S2. Nb K-edge extended X-ray absorption fine structure (EXAFS) fit for different coordination models in R-space and q-space for **(a)** pristine N_0NbP, **(b)** after 10th cycle of N_0NbP anodes cycled in 3.0 V – 1.1 V and **(c)** 3.0 V – 1.0 V potential window.

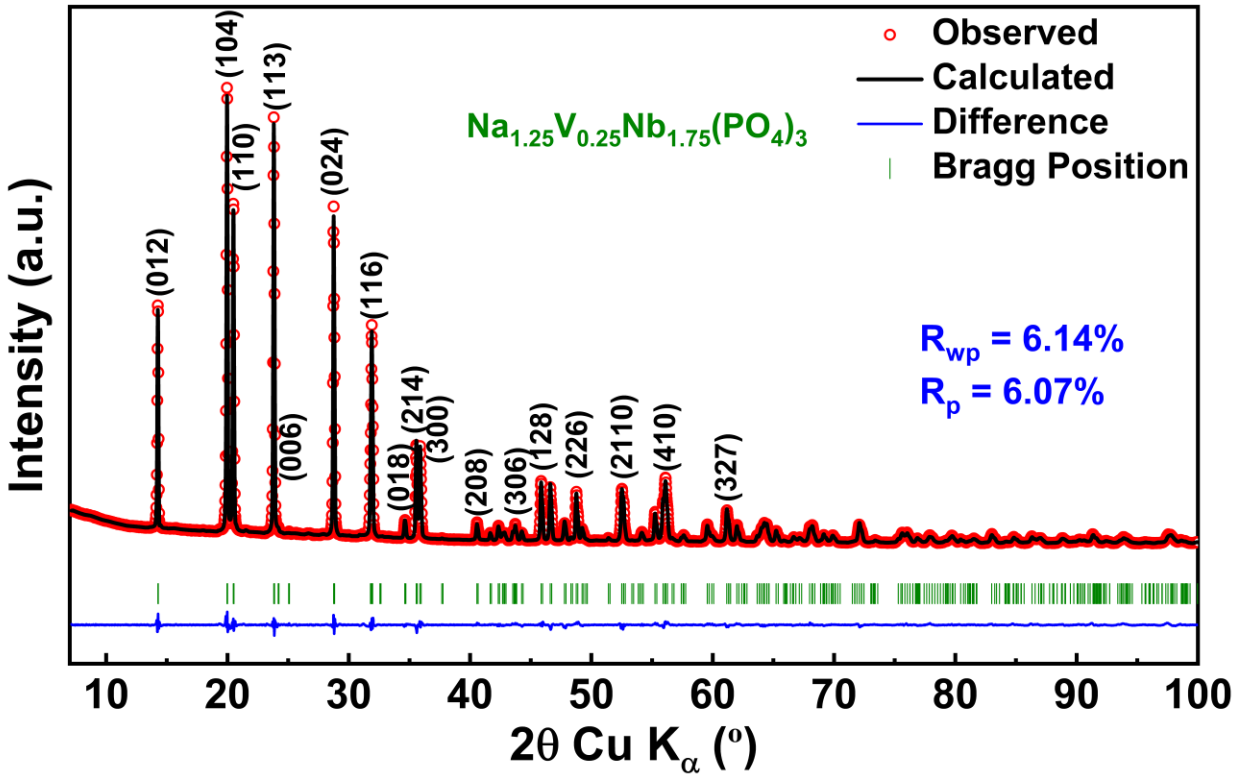

Figure S3. Rietveld refinement of XRD pattern collected on the $Na_{1.25}V_{0.25}Nb_{1.75}(PO_4)_3$ ($N_{1.25}$VNbP) anode.

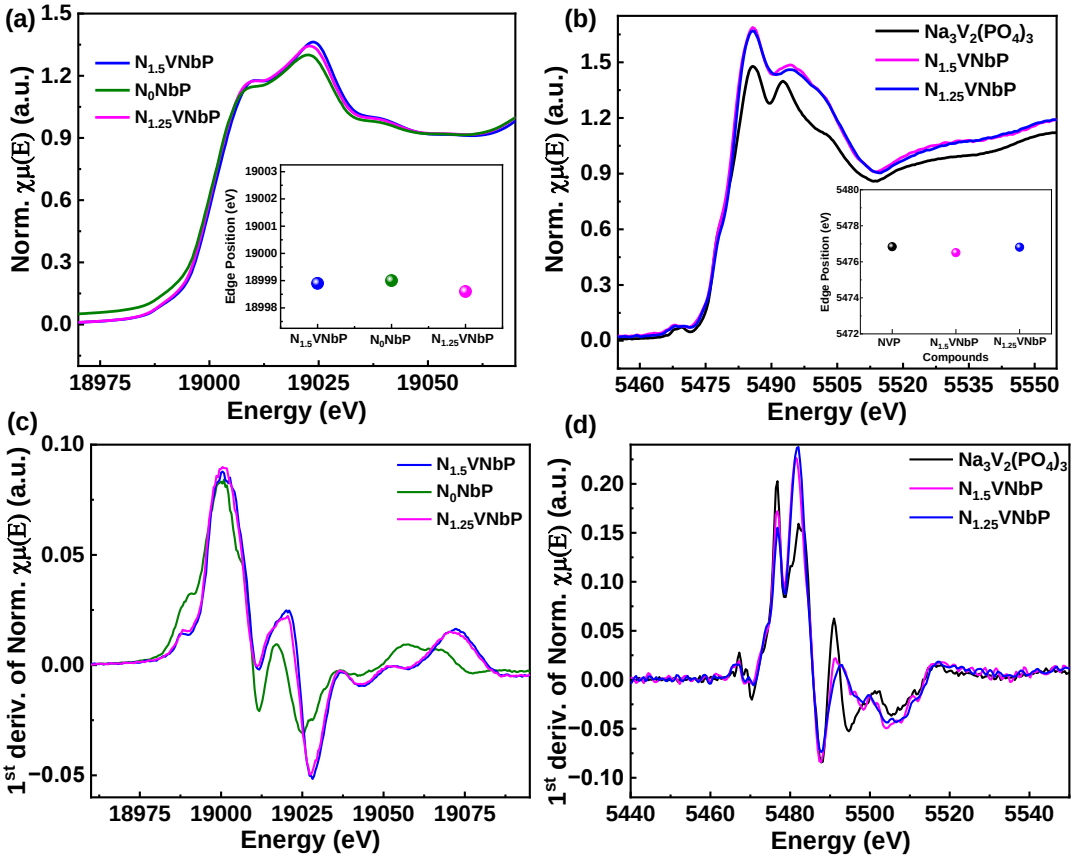

Figure S4. Normalized X-ray absorption near edge structure (XANES) spectra of N_0NbP, $N_{1.25}$VNbP, and $N_{1.5}$VNbP compounds at (a) Nb and (c) V K-edges, the edge position determined by the first inflection point of the derivative spectra (b) Nb and (d)V K-edge. The colour code in the inset belongs to the spectra. $Nb_2(PO_4)_3$ and $Na_3V_2(PO_4)_3$ taken as Nb and V standard.

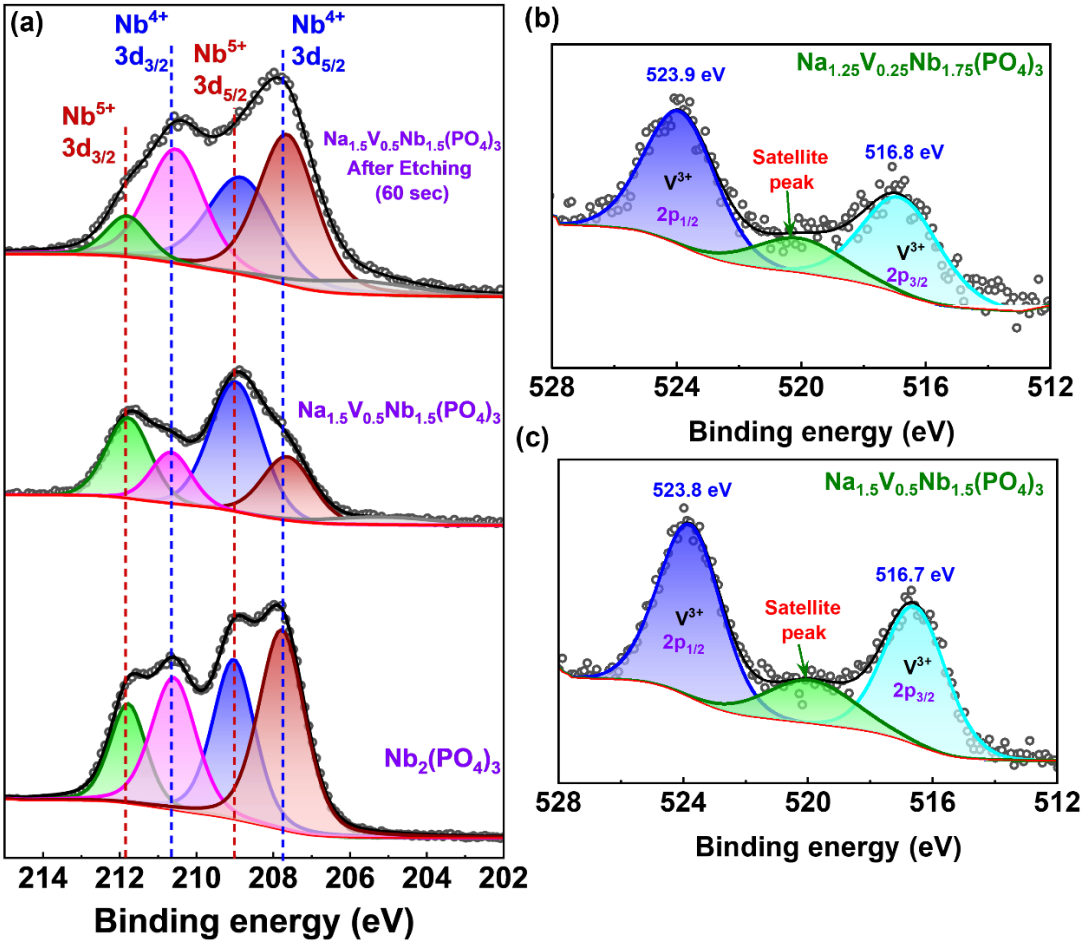

Figure S5. X-ray photoelectron spectroscopy (XPS) spectra of (a) Nb3d for N_0NbP, and $N_{1.5}$VNbP, (b) V2p for $N_{1.5}$VNbP and $N_{1.5}$VNbP.

The X-ray photoelectron spectroscopy (XPS) spectra of N_0NbP composed of Nb-$3d_{3/2}$ and Nb-$3d_{5/2}$ peaks located at 211.7 eV and 208.7 eV suggesting Nb^{5+}, whether the peak at 210.7 eV and 207.8 eV indicates the presence of Nb^{4+}. This result confirms the mixed valence of Nb in N_0NbP. Similar peak observed in case of $N_{1.5}$VNbP with different proportion in the surface indicating the surface oxidation of Nb^{5+} and the peak intensity decreases after etching which corresponds the presence of Nb^{4+} in bulk. The V 2p spectra is made up of two primary single peaks. at 517.0 eV (V-$2p_{3/2}$) and 523.8 eV (V-$2p_{1/2}$) with a satellite peak shown in Fig. S9b, suggesting the existence of V^{3+} in both $N_{1.5}$VNbP and $N_{1.25}$VNbP samples.

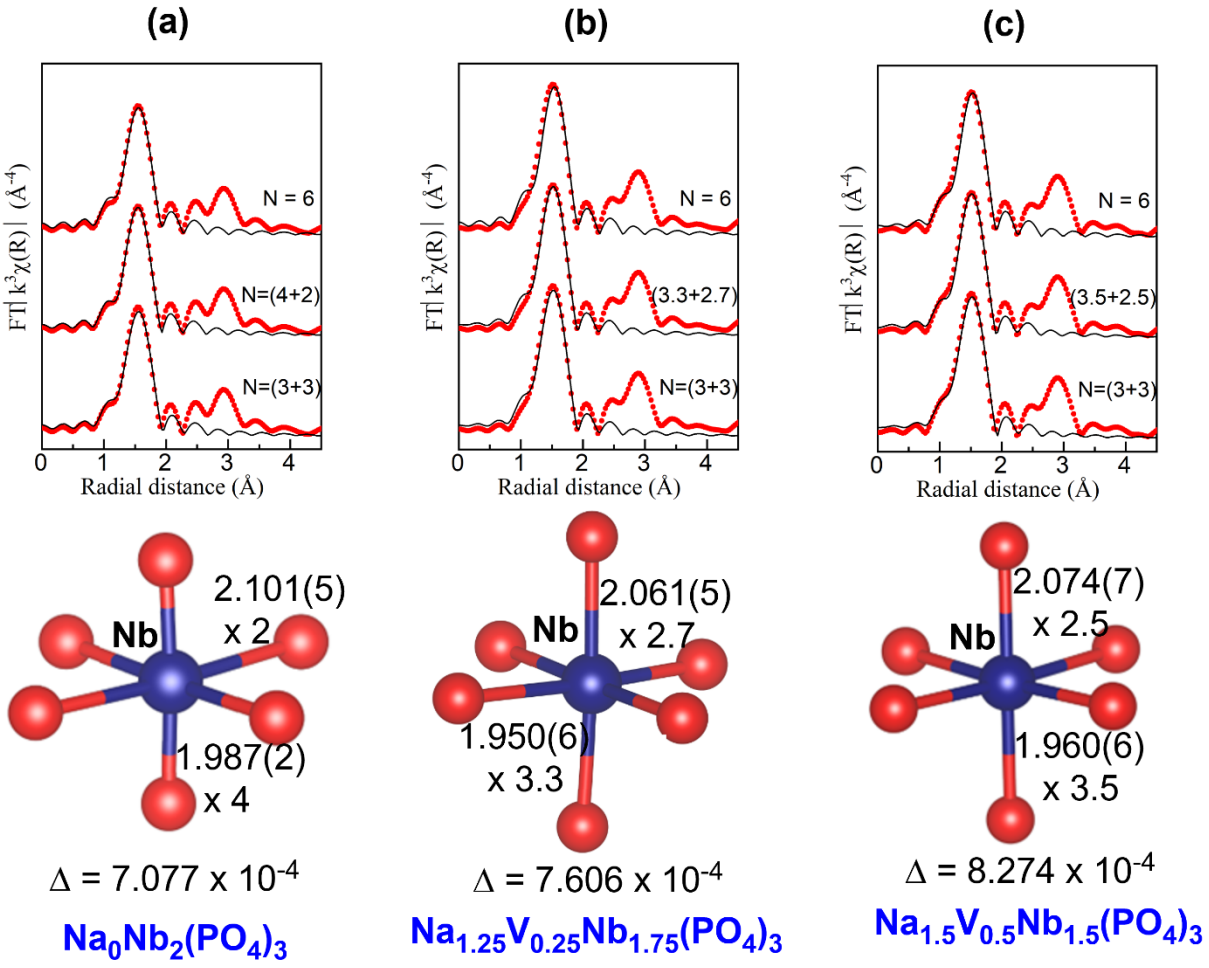

Figure S6. Nb K-edge EXAFS fits with different coordination models in R-space and the local environment of NbO_6 for as-synthesized **(a)** N_0NbP, **(b)** $Na_{1.25}$VNbP, and **(c)** $Na_{1.5}$VNbP anodes.

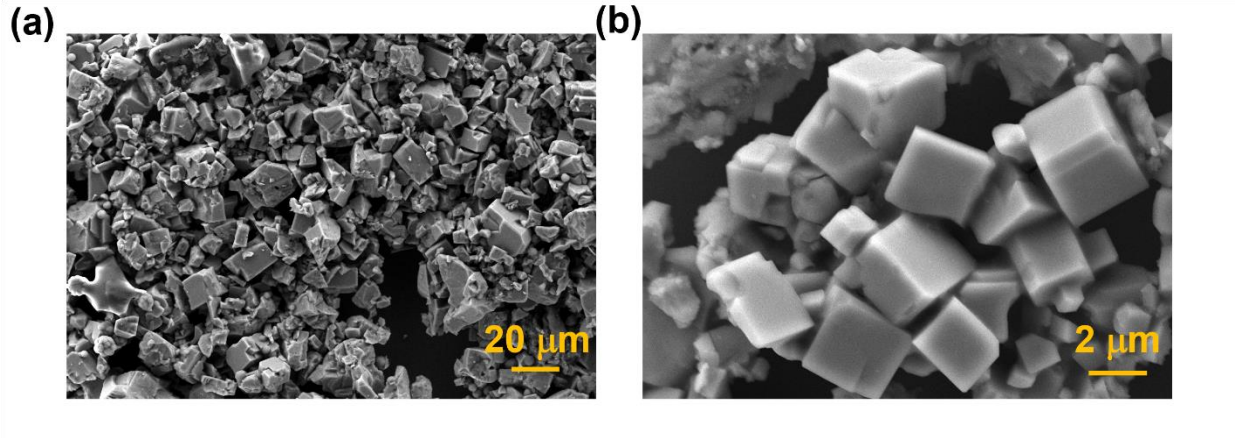

Figure S7. (a,b) SEM images of $N_{1.25}$VNbP at different scales.

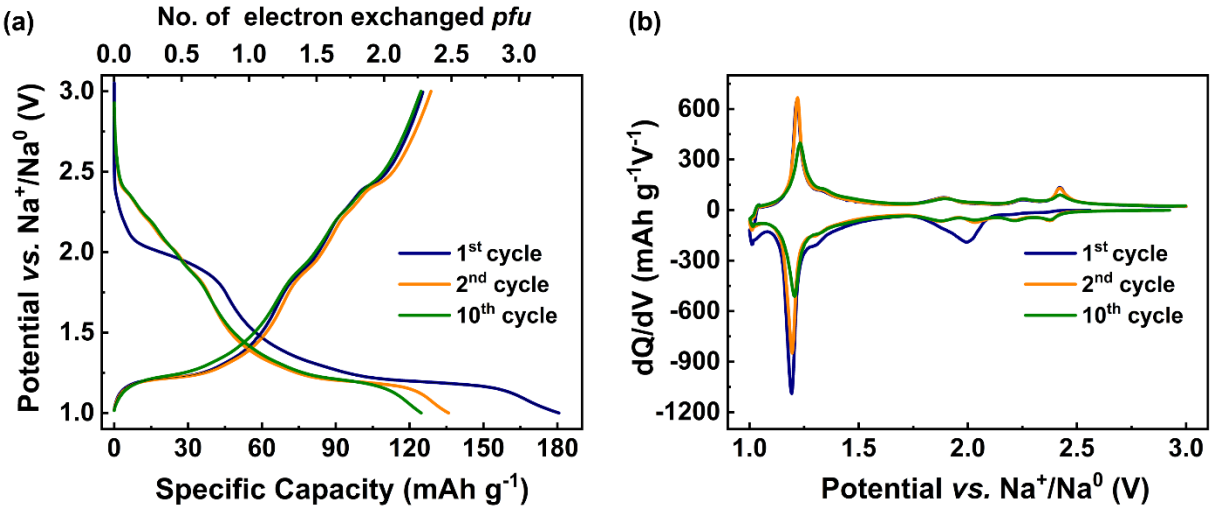

Figure S8. (a) Voltage-capacity and (b) dQ/dV profiles of $N_{1.25}$VNbP anode.

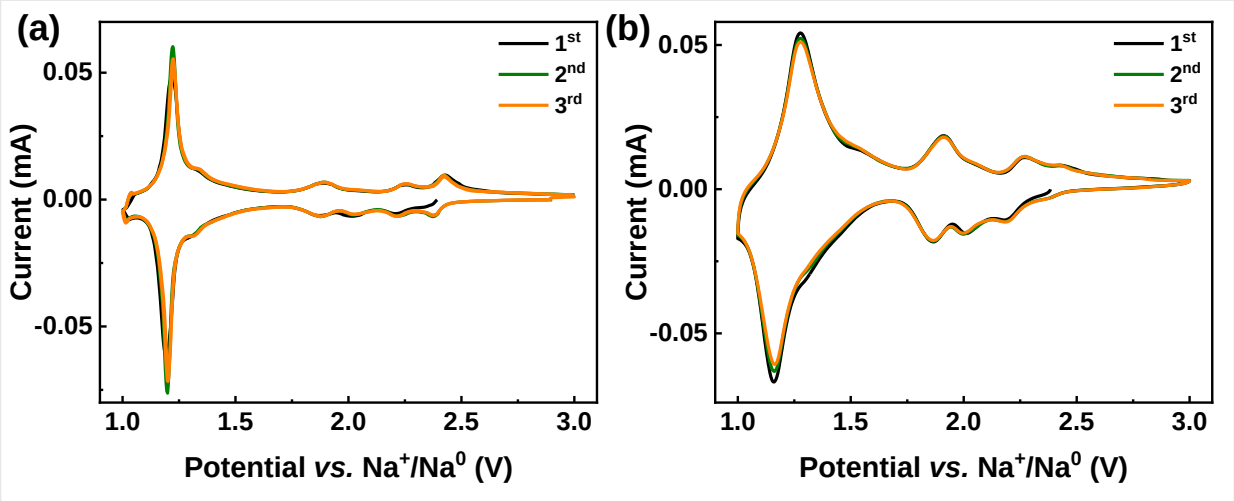

Figure S9: CV profiles of (a) $N_{1.25}VNbP$ and (b) $N_{1.5}VNbP$ anodes at a scan rate of 0.05 mV s^{-1}.

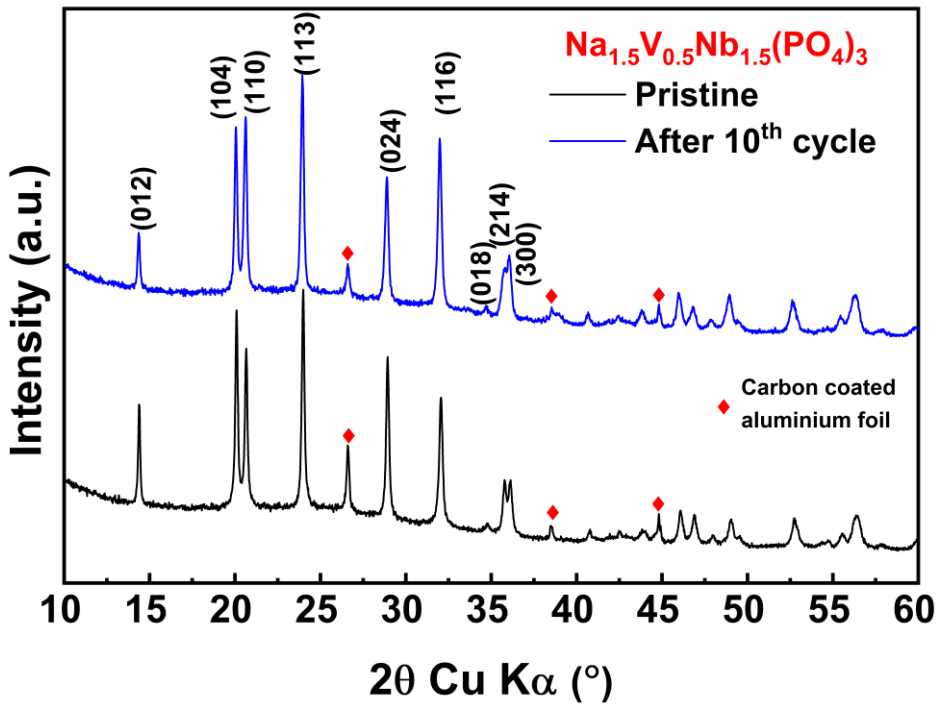

Figure S10. XRD patterns of pristine and cycled $N_{1.5}VNbP$ anodes.

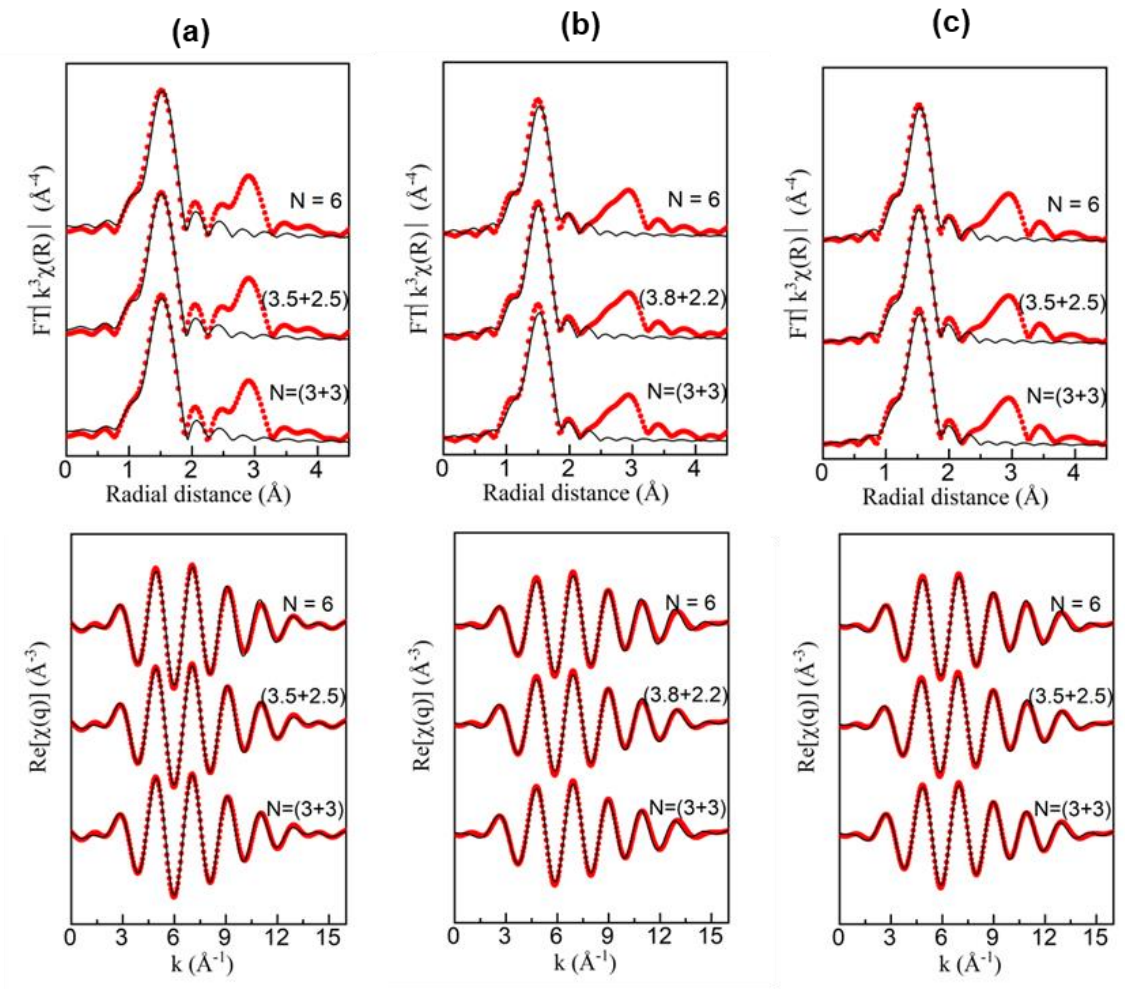

Figure S11. Nb K-edge EXAFS fit for different coordination models in R-space and q-space for **(a)** pristine, **(b)** after 1st cycle and **(c)** after 10th cycle of $Na_{1.5}VNbP$ electrode.

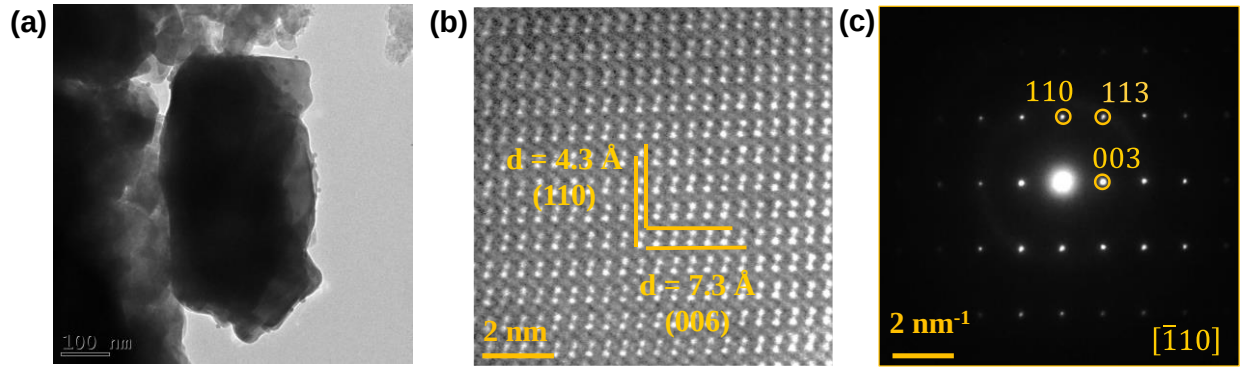

Figure S12. (a) Low magnification TEM image, (b) HRTEM image, and (c) SAED pattern of the $N_{1.5}VNbP$ anode collected after the 10th cycle.

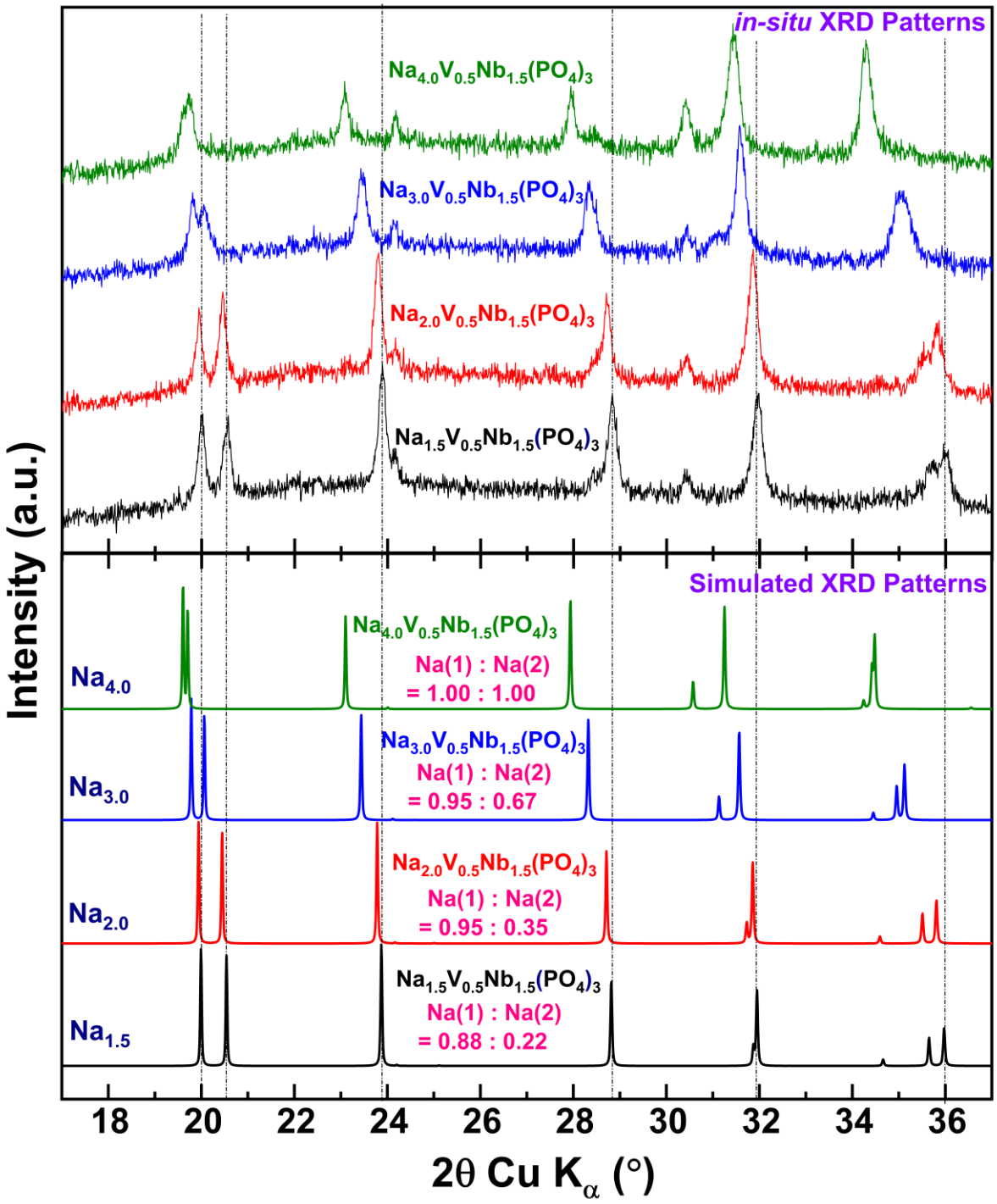

Figure S13. Comparison of selected *in-situ* and simulated XRD patterns.

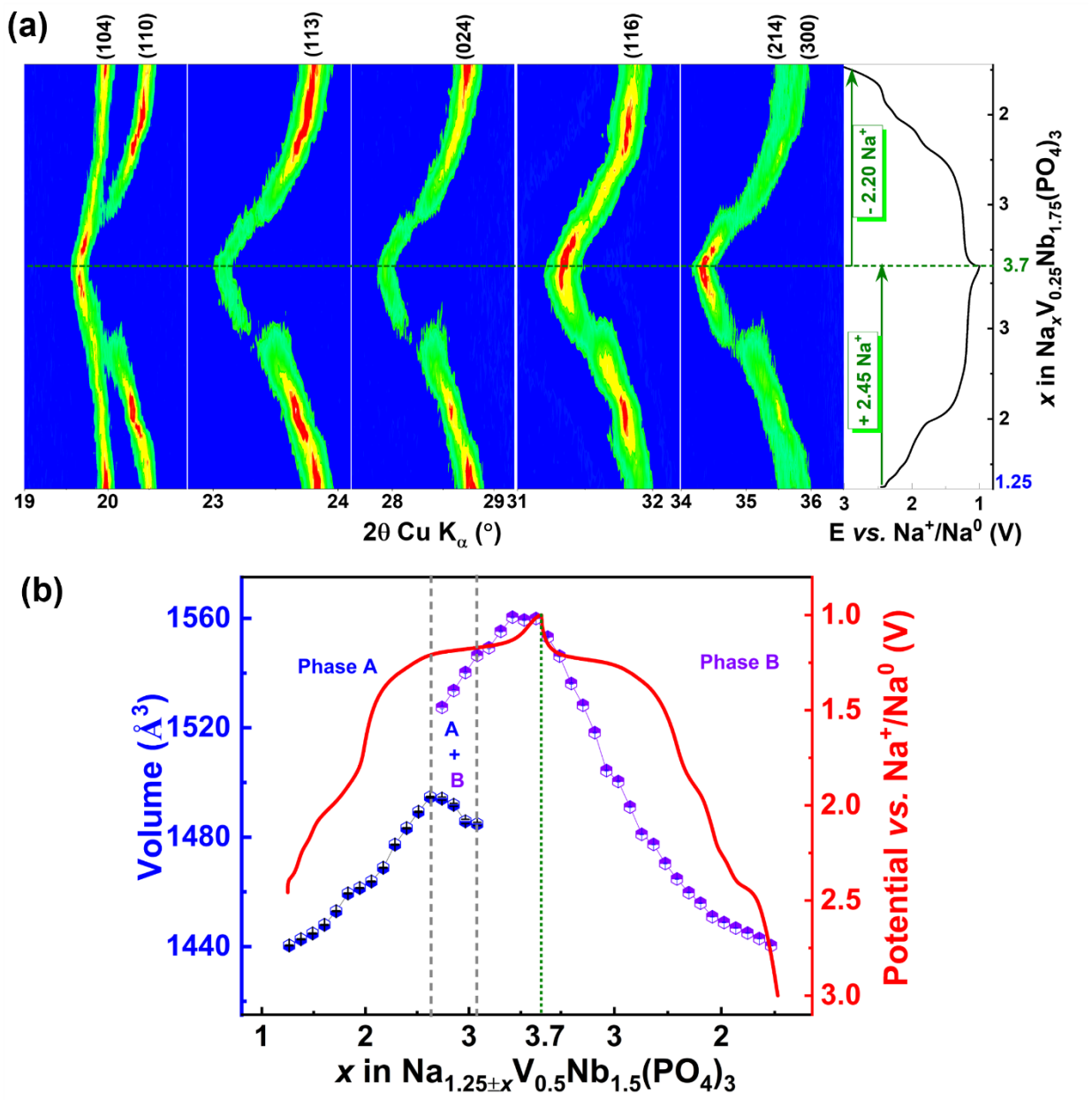

Figure S14. (a) Intensity contour map of *in-situ* XRD patterns and (b) evolution of unit cell volume of $N_{1.25}$VNbP anode during the second cycle.

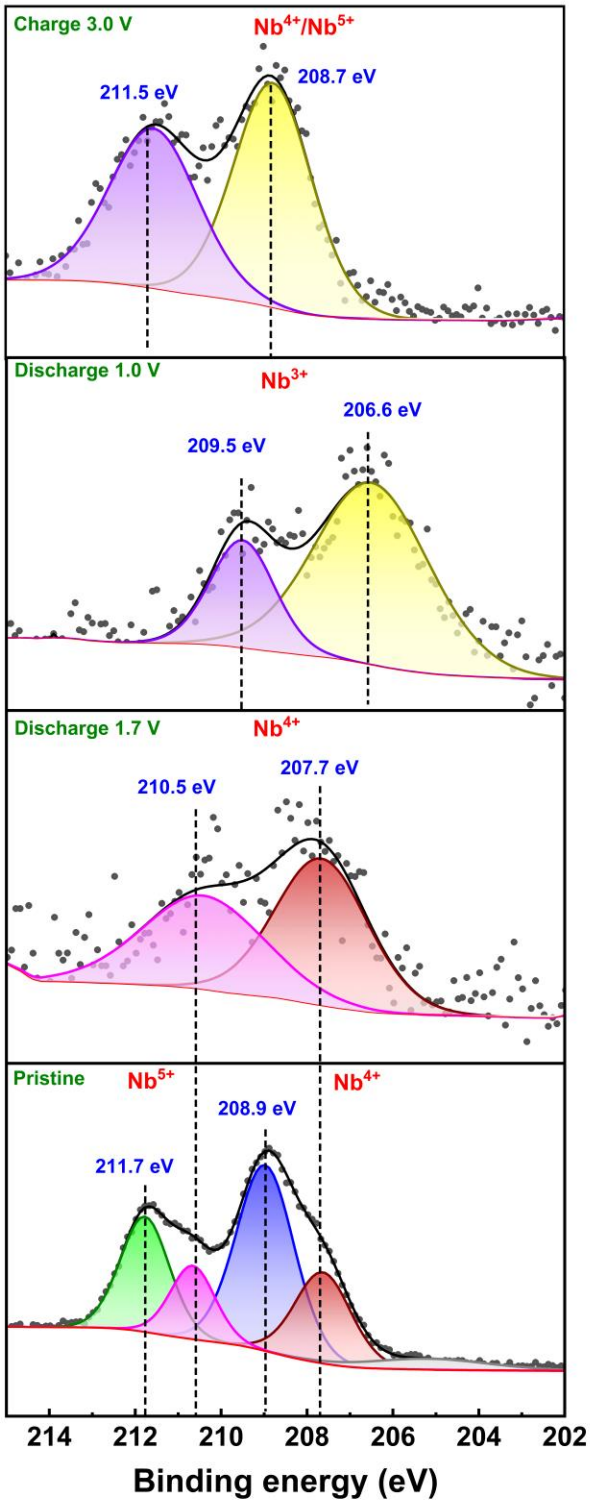

Figure. S15. Ex-situ XPS spectra of Nb3d during cycling for $N_{1.5}$VNbP

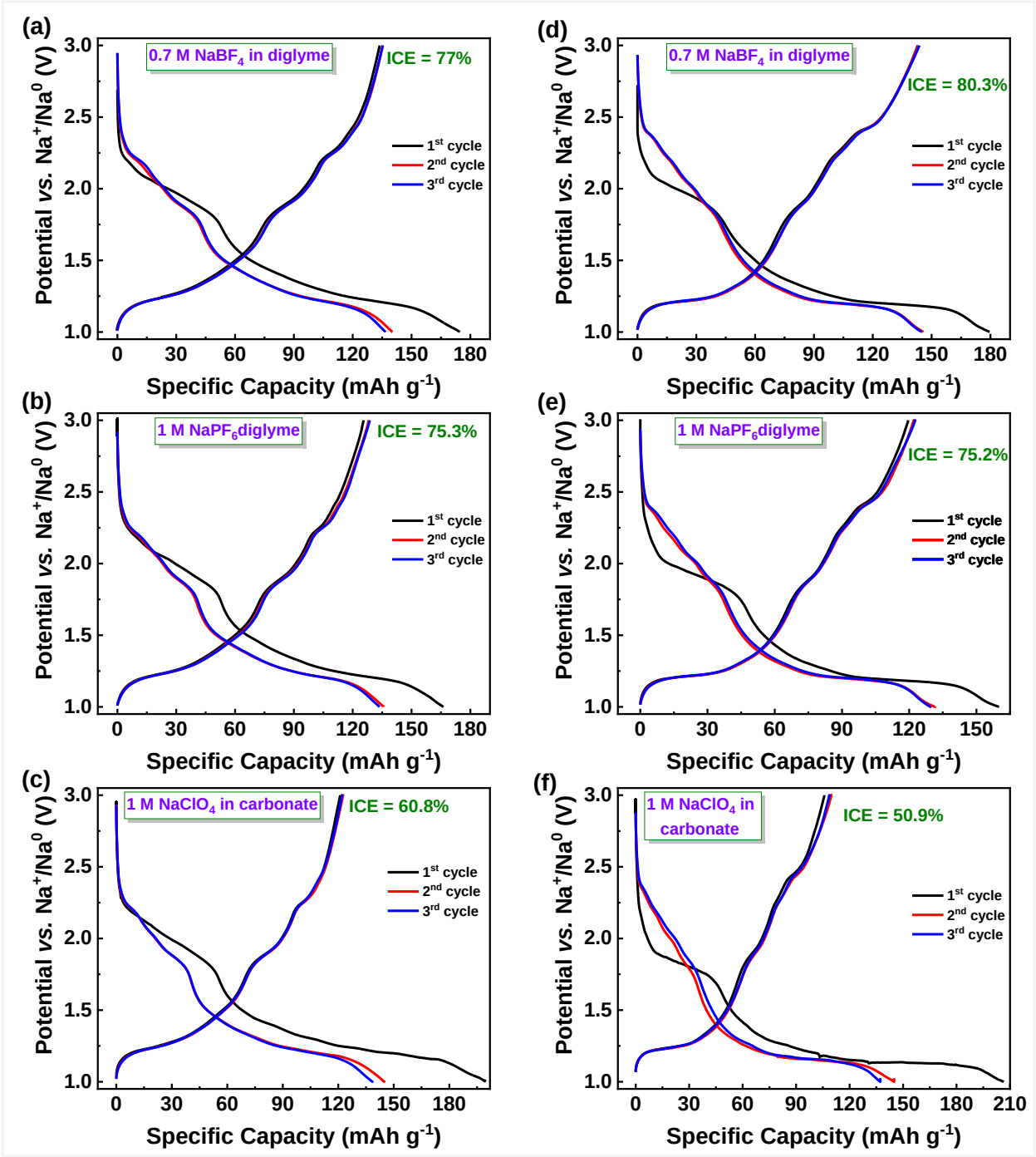

Figure S16. Voltage-capacity plots at C/5 rate in different electrolyte systems (a-c) $N_{1.5}$VNbP, (d-f) $N_{1.25}$VNbP

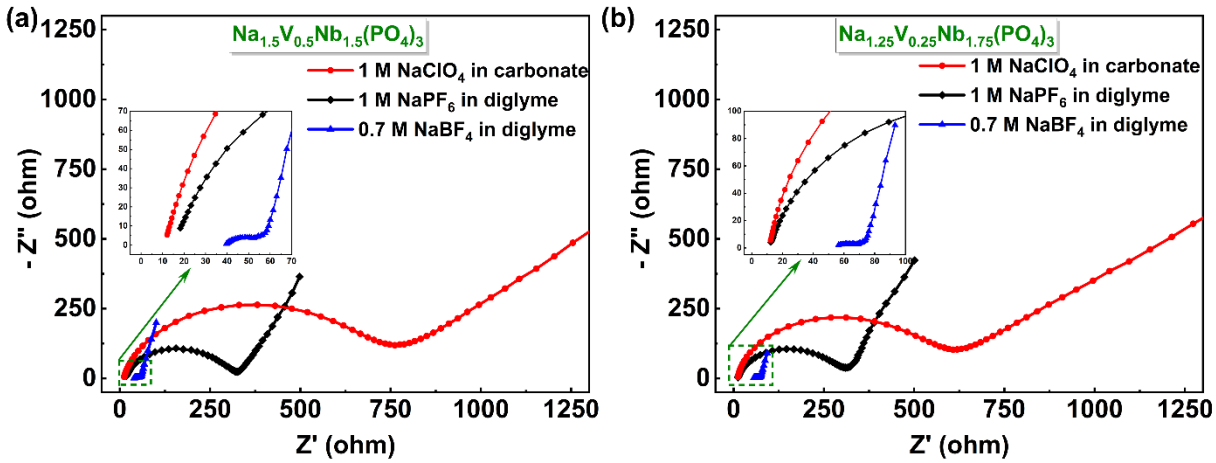

Figure S17. Pristine impedance comparison for $Na_{1.5}$VNbP and $Na_{1.25}$VNbP in different electrolytes.

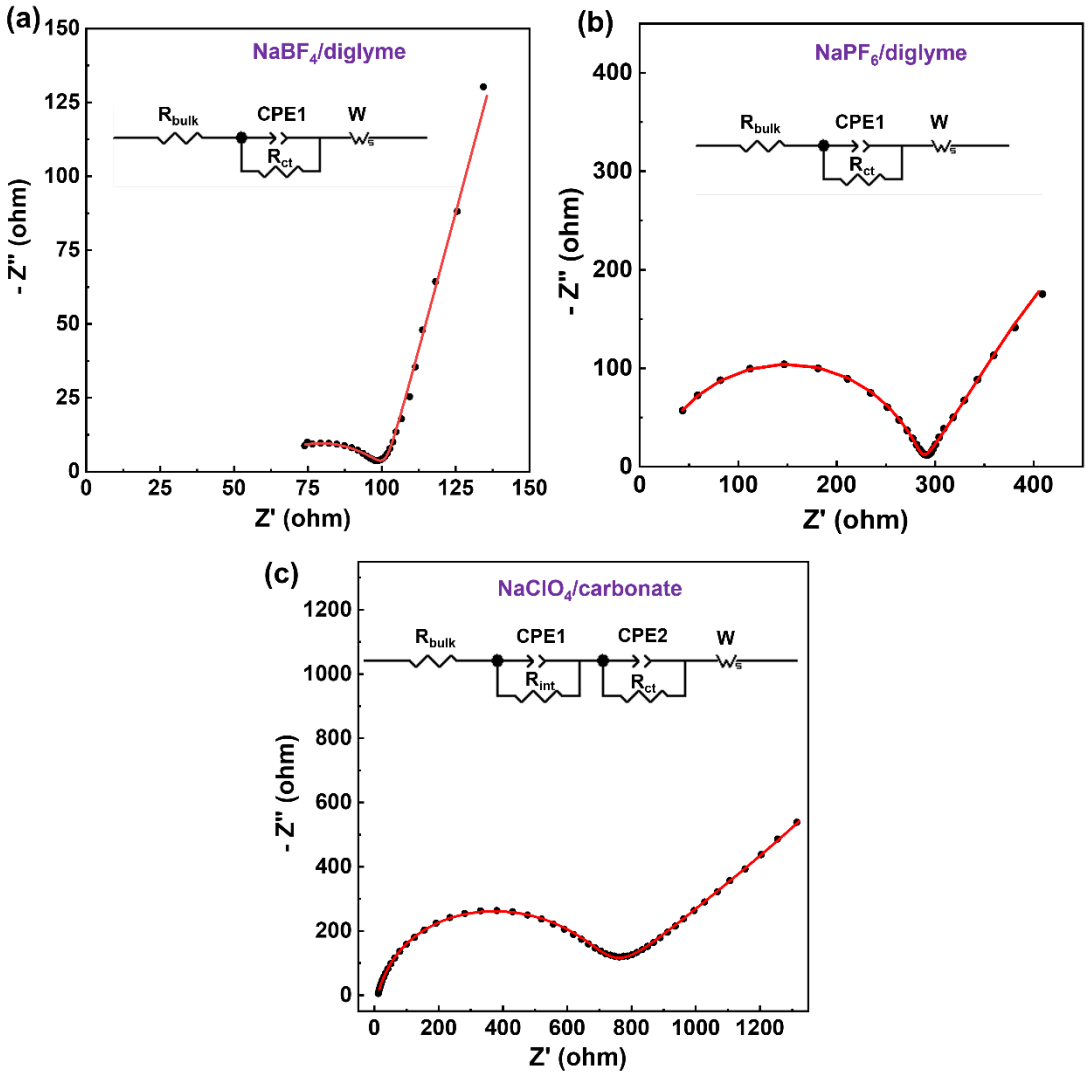

Figure S18. Equivalent circuit model for fitting Nyquist plots of electrochemical impedance spectroscopy (EIS) measurements in different electrolytes for $N_{1.5}VNbP$. R_{bulk}, R_{int} and R_{ct} denote the ion transport in bulk electrolyte, interfacial resistance between electrode and electrolyte and charge transfer resistance, respectively. CPE1 and CPE2 are the constant phase elements. W is the Warburg element that represents solid state diffusion.

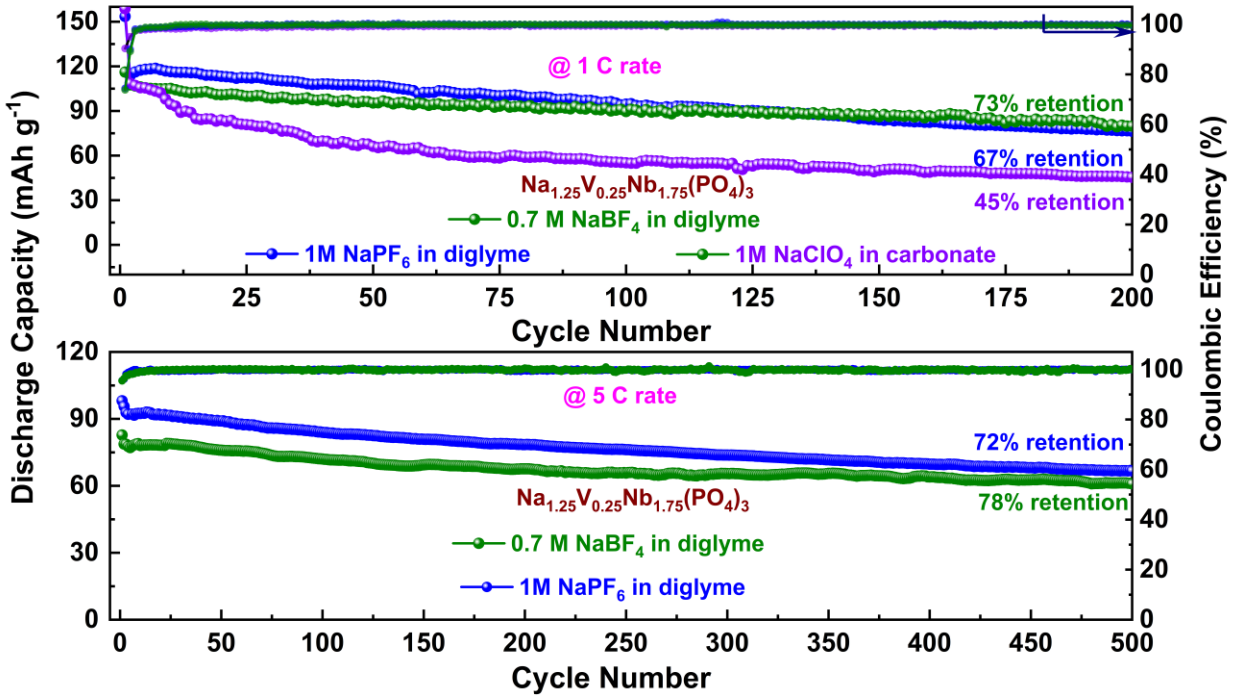

Figure S19. Long-term cycling stability of the $N_{1.25}$VNbP electrode at 1 C and 5 C rates.

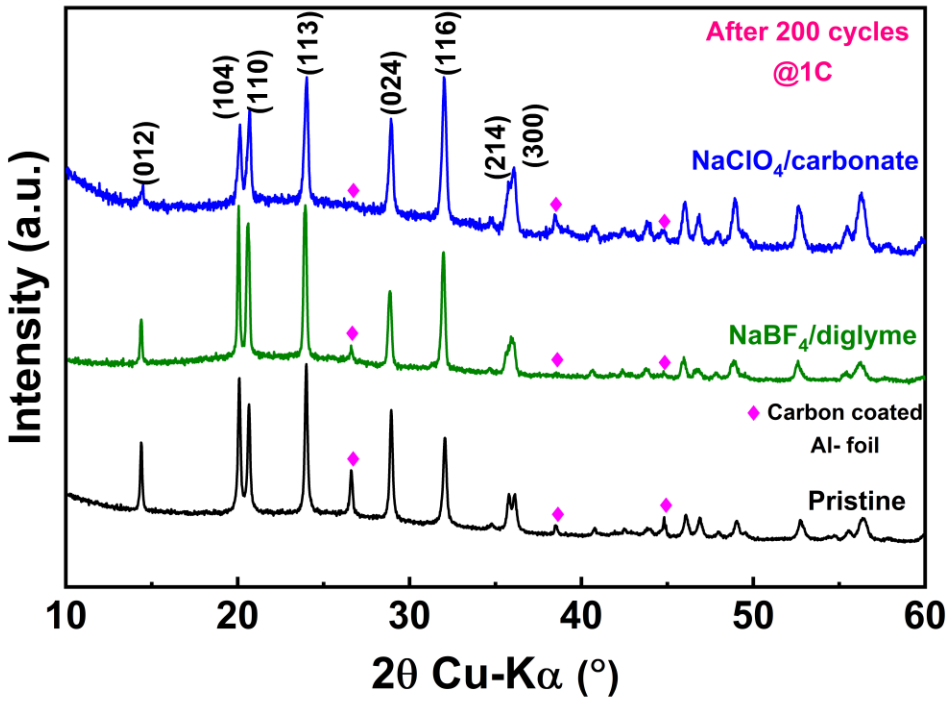

Figure S20. XRD patterns of pristine and cycled $Na_{1.5}$VNbP anodes in different electrolytes.

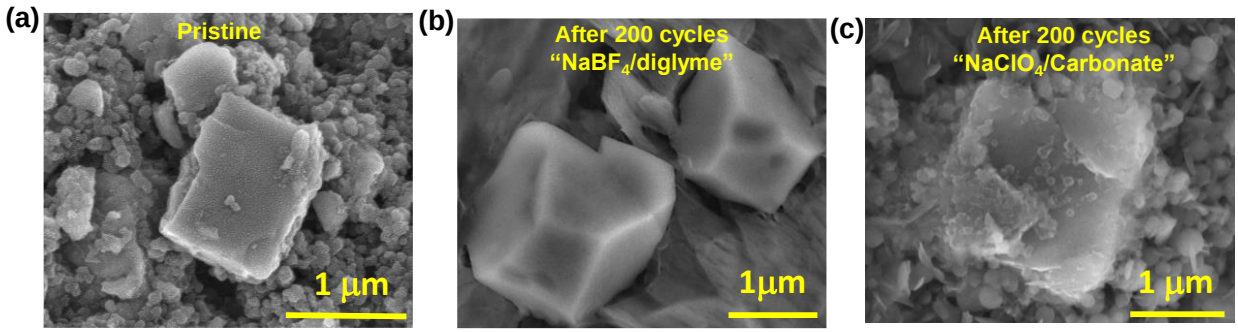

Figure S21. SEM images of (a) pristine and (b,c) cycled $N_{1.5}$VNbP anodes in different electrolytes.

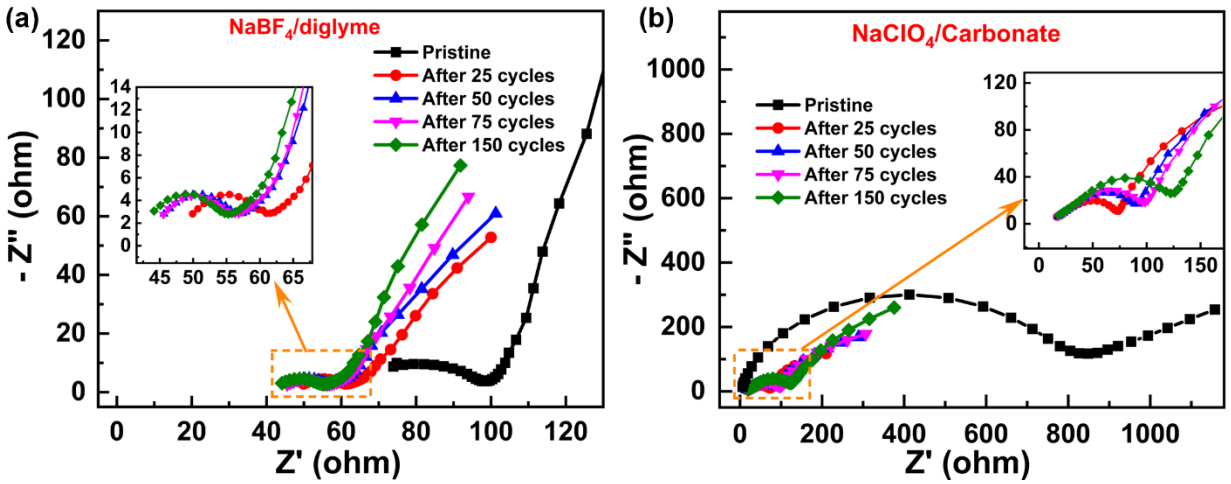

Figure S22. Electrochemical impedance spectroscopy (EIS) spectra of $Na_{1.5}$VNbP collected at different cycles in (a) $NaBF_4$/diglyme and (b) $NaClO_4$/carbonate electrolyte.

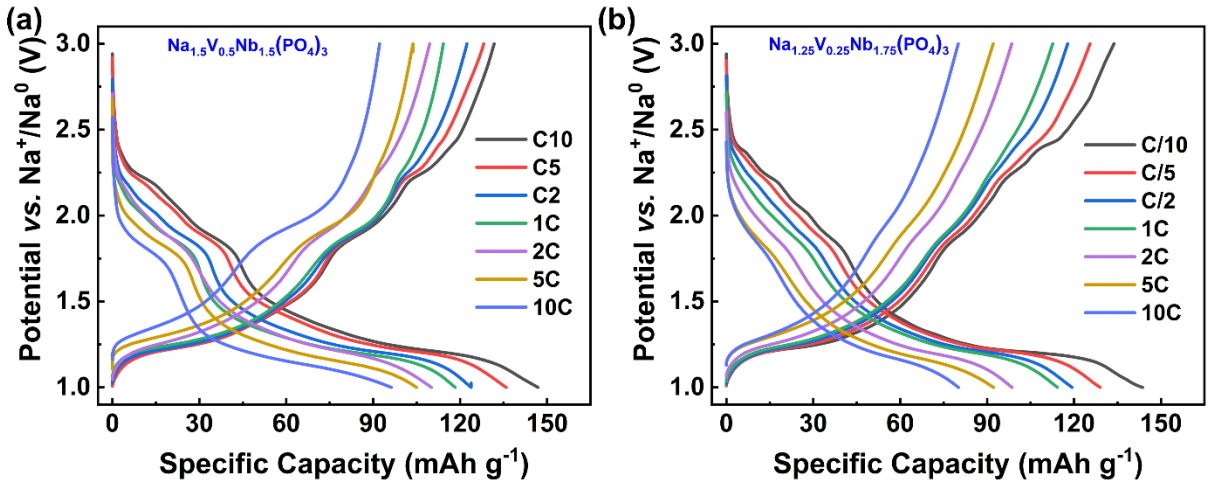

Figure S23. Voltage vs. capacity profiles of $Na_{1.5}$VNbP and $Na_{1.25}$VNbP anode collected at different C-rates.

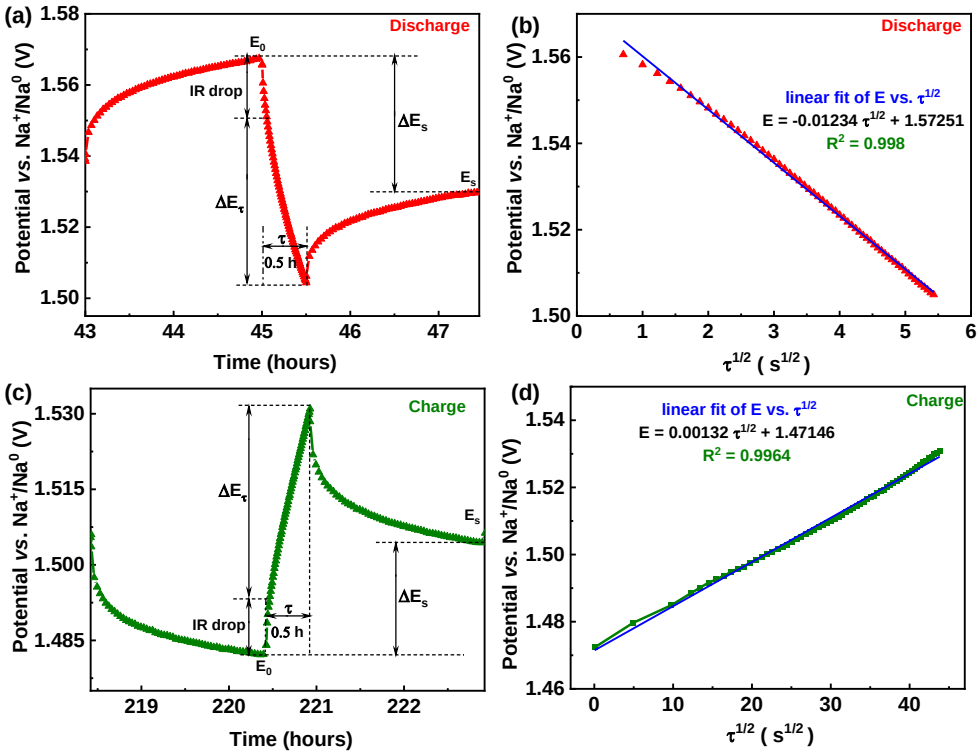

Figure S24. Potential vs. time curves of the $N_{1.5}VNbP$ anode for a single step galvanostatic intermittent titration technique (GITT) experiment during (a) discharge, and (c) charge processes at C/10 rate and their corresponding linear fitted plot of potential vs. $\tau^{1/2}$ for the (b) discharge and (d) charge processes.

The Na diffusion kinetics of $N_{1.5}VNbP$ was investigated by galvanostatic intermittent titration technique (GITT) after 3 cycles when it obtain the equilibrium state. During the experiment, the cell was charged and discharged at C/10 rate for 0.5 h followed by relaxation of 2 h to allow the voltage to reach equilibrium and this process was repeated to the cell during the entire cycle. The sodium-ion diffusivity (D_{Na+}) values can be determined according to the equation established by Weppner and Huggins[1]:

$$D_{Na^+} = \frac{4}{\pi\tau}\left(\frac{m_B V_M}{M_B A}\right)^2 \left(\frac{\Delta E_s}{\Delta E_\tau}\right)^2 \qquad \left(\tau \ll \frac{L^2}{D_{Na^+}}\right)$$

The parameters involved in the above equation are explained below,

τ = time of constant current pulse (1800 s), m_B = mass of the active material (g), M_B = molecular weight (g mol^{-1}), V_M = molar volume (cm^3 mol^{-1}), A = total contacting area of electrode with electrolyte (cm^2). ΔE_s = Difference between the voltage during the open circuit period, ΔE_τ = total change of cell voltage during a constant current pulse excluding the resistance (IR) drop, and L = average radius of the active material particles.

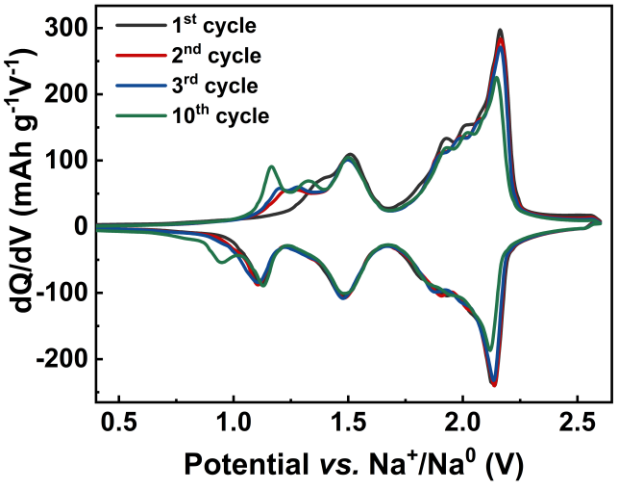

Figure S25. dQ/dV profile for $N_{1.5}$VNbP||NVP Full cell

Table S1. Lattice parameters obtained from the Le-Bail fitting of powder XRD patterns of pristine and cycled N_0NbP electrodes.

$Nb_2(PO_4)_3$, space group: $R\bar{3}c$ (#167); Z = 6			
	a (Å)	c (Å)	V ($Å^3$)
Pristine	8.68438	22.0926	1442.962
3.0 V- 1.1 V	8.68136	22.27101	1453.604
3.0 V - 1.0 V	8.68994	22.59892	1477.922

Table S2. Refined parameters for the first shell of EXAFS spectra collected at Nb K-edge of the pristine N_0NbP and after 10^{th} cycle in different voltage window.

k-range: 2.6 – 13 $Å^{-1}$**, dk** = 1.0**, window:** hanning					
(a) Pristine N_0NbP					
Coordination	**d(Nb-O) Å**	**S^2_0**	**E_0 (eV)**	**σ^2 $Å^2$**	**R-factor**
6	2.011(5) x 6	0.72(8)	4.3(7)	0.0034(8)	0.0154
3 + 3	1.968(4) x 3 2.069(4) x 3	0.72(8)	5.1(6)	0.0006(6)	0.0113
4 + 2	1.987(2) x 4 2.101(5) x 2	0.72(8)	5.42(1.04)	0.0005(8)	0.0090
(b) After 10^{th} cycle (3.0 V- 1.1 V window)					
6	2.018(2) x 6	0.63(4)	2.2(9)	0.004(1)	0.0225
3 + 3	1.971(4) x 3 2.084(8) x 3	0.63(4)	3.2(7)	0.0002(7)	0.0148
3.6 + 2.4	2.098(8) x 2.4 1.98362 x 3.6	0.63(4)	3.1(7)	0.0003(3)	0.0142
(c) After 10^{th} cycle (3.0 V - 1.0 V window)					
6	2.030(3) x 6	0.7(1)	-2.41(1.6)	0.008(8)	0.1590
3 + 3	2.031(5) x 3 2.039(6) x 3	0.7(1)	-0.5(1)	0.008(1)	0.184
5 + 1	2.031(4) x 5 1.715(5) x 1	0.7(1)	-1.6(8)	0.006(1)	0.0135

Table S3. Crystallographic parameters obtained from the Rietveld refinements of **(a)** $Na_{1.5}VNbP$ and **(b)** $Na_{1.25}VNbP$.

(a) $Na_{1.5}V_{0.5}Nb_{1.5}(PO_4)_3$, space group: $R\bar{3}c$ (#167); Z = 6						
a = 8.6368(7) Å; c = 22.0647(3) Å; c/a = 2.554; V = 1425.16(3) Å^3; V/Z = 237.526(7) Å^3						
R_{wp} = 8.12%; R_p = 8.79%; R_{Bragg} = 7.40%						
Atom	Wyckoff	x	y	z	Uiso, Å^2	Occ.
Nb	12c	0	0	0.14244(4)	0.00033(17)	0.75
V	12c	0	0	0.14244(4)	0.00033(17)	0.25
P(1)	18e	0.2835(2)	0	0.25	0.013(5)	1.0
Na(1)	6b	0	0	0	0.172(11)	0.758(4)
Na(2)	18e	0.6320(1)	0	0.25	0.5454(1)	0.212(4)
O(1)	36f	0.0296(4)	0.2070(3)	0.19364(14)	0.011(11)	1.0
O(2)	36f	0.1974(3)	0.1692(3)	0.08727(12)	0.0009(9)	1.0
(b) $Na_{1.25}V_{0.25}Nb_{1.75}(PO_4)_3$, space group: $R\bar{3}c$ (#167); Z = 6						
a = 8.6646(4) Å; c = 22.066(2) Å; c/a = 2.546; V = 1434.730(2) Å^3; V/Z = 239.121(2) Å^3						
R_{wp} = 6.14%; R_p = 6.07%; R_{Bragg} = 2.67%						
Atom	Wyckoff	x	y	z	Uiso, Å^2	Occ.
Nb	12c	0	0	0.1416(5)	0.0108(2)	0.875
V	12c	0	0	0.1416(5)	0.0108(2)	0.125
P(1)	18e	0.2823(2)	0	0.25	0.0133(5)	1.0
Na(1)	6b	0	0	0	0.965(2)	0.829(2)
Na(2)	18e	0.7810(2)	0	0.25	0.670(1)	0.113(6)
O(1)	36f	0.0348(4)	0.2041(4)	0.1923(1)	0.021(3)	1.0
O(2)	36f	0.2000(1)	0.1683(3)	0.0916(1)	0.0074(8)	1.0

Table S4. Average O(2)-O(2) distances obtained from the Rietveld refinement.

Sample	O2-O2 (Å)
N_0NbP	4.1968
$Na_{1.25}VNbP$	4.0320
$Na_{1.5}VNbP$	3.8682

Table S5. Refined parameters for the first shell of EXAFS spectra at Nb K-edge of pristine $N_{1.25}$VNbP anode.

k-range: 2.6 – 13 Å^{-1}**, dk** = 1.0**, window:** hanning					
$Na_{1.25}V_{0.25}Nb_{1.75}(PO_4)_3$					
6	2.000(8) x 6	0.8(1)	2.9(2.7)	0.003(1)	0.0218
3 + 3	1.941(5) x 3 2.051(4) x 3	0.8(1)	2.2(8)	0.0007(5)	0.0173
3.3 + 2.7	1.950(6) x 3.3 2.061(5) x 2.7	0.8(1)	2.7(9)	0.0004(5)	0.0153

Table S6. Refined parameters for the first shell of EXAFS spectra for Nb K-edge of the (a) pristine $Na_{1.5}$VNbP, (b) after 1st cycle and (c) after 10th cycle.

k-range: 2.6 – 13 Å^{-1}**, dk** = 1.0**, window:** hanning					
(a) Pristine $Na_{1.5}V_{0.5}Nb_{1.5}(PO_4)_3$					
Coordination	**d(Nb-O) Å**	**S^2_0**	**E_0 (eV)**	**σ^2 Å^2**	**R-factor**
6	1.988(9) x 6	0.8(1)	4.02(2.0)	0.0039(9)	0.0146
3 + 3	1.935(3) x 3 2.047(6) x 3	0.8(1)	4.2(1.90	0.0001(6)	0.0110
3.5 + 2.5	1.949(8) x 3.5 2.066(4) x 2.5	0.8(1)	4.94 (2.3)	0.0002(5)	0.0087
(b) After 1st cycle					
6	1.991(7) x 6	0.70(9)	-1.1(2.1)	0.003(1)	0.0231
3 + 3	1.9440(8) x 3 2.049(2) x 3	0.70(9)	-0.53(1.0)	0.0003(8)	0.0199
3.8 + 2.2	1.960(4) x 3.8 2.073(7) x 2.2	0.70(9)	-0.2(8)	0.0003(9)	0.0168
(c) After 10th cycle					
6	1.996(8)	0.70(9)	2.0(1.5)	0.003(8)	0.0125
3 + 3	1.946(3) x 2.049(6) x 3	0.70(9)	2.0(1.5)	0.0005(6)	0.0095
3.5 + 2.5	1.958(1) x 3.5 2.065(2) x 2.5	0.70(9)	2.4(1.5)	0.0005(6)	0.00884

Table S7. Fitted parameters from EIS of $Na_{1.5}VNbP$|Na cell cycled in different electrolytes.

Electrolyte	**Pristine**			**After 25 cy**			**After 50 cy**			**After 75 cy**			**After 150cy**		
	R_{bulk}	R_{int}	R_{ct}	R_{bulk}	R_{int}	R_{ct}	R_{bulk}	R_{int}	R_{ct}	R_{bulk}	R_{int}	R_{ct}	R_{bulk}	R_{int}	R_{ct}
$NaBF_4$/ diglyme	57.06	-	44.67	46.46	-	16.62	41.95	-	17.02	39.79	-	20.59	36.27	-	20.97
$NaPF_6$/ diglyme	11.47	-	274.8	14.22	-	7.235	15.55	-	8.13	10.65	-	14.95	9.423	-	16.91
$NaClO_4$/ carbonate	8.976	282.3	393.9	10.43	30.13	30.28	10.74	38.63	41.25	10.77	42.43	44.61	9.767	47.89	64.93

Table S8. Comparison full Na-ion cells comprising NASICON materials as cathode and anode.

Cathode || Anode	Capacity, Current density	Average Voltage	Capacity retention	Rate performance	Energy Density		Ref
					Based on Cathode	Based on Cathode + Anode	
$Na_3V_2(PO_4)_3$ || $NaTi_2(PO_4)_3$	128 mAh g^{-1}, 13.3 mA g^{-1}	1.2 V	80% after 1000 cycles, at 1.33 A g^{-1}	90 mAh g^{-1} at 6.65 A g^{-1}	-	73 Wh kg^{-1}	[2]
$Na_3V_2(PO_4)_3$ || $Na_3V_2(PO_4)_3$	100 mAh g^{-1}, 58.8 mA g^{-1}	1.7 V	75% after 200 cycles, at 0.117 A g^{-1}	42 mAh g^{-1} at 1.176 A g^{-1}	185.5 Wh kg^{-1}	-	[3]
$Na_3V_2(PO_4)_3$|| $Na_3V_2(PO_4)_3$	90.2 mAh g^{-1}, 29 mA g^{-1}	1.7 V	71% after 280 cycles at 234 mA g^{-1}	34 mAh g^{-1} at 1.176 A g^{-1}	162 Wh kg^{-1}	-	[4]
$Na_2VTi(PO_4)_3$ || $Na_2VTi(PO_4)_3$	72 mAh g^{-1}, 125 mA g^{-1}	1.2 V	74% after 10000 cycles at 1.25 A g^{-1}	49 mAh g^{-1} at 2.5 A g^{-1}	-	33.2 Wh kg^{-1}	[5]
$Na_3V_2(PO_4)_3$|| $NaTi_2(PO_4)_3$	103 mAh g^{-1}, 117 mA g^{-1}	1.2 V	96.9% after 300 cycles at 0.585 A g^{-1}	80 mAh g^{-1} at 5.85 A g^{-1}	90 Wh kg^{-1}	58 Wh kg^{-1}	[6]
$Na_3V_2(PO_4)_3$|| $N_{1.5}VNbP$	104 mAh g^{-1}, 11.7 mA g^{-1}	1.9 V	80 % after 1000 cycles at 0.585 A g^{-1}	70 mAh g^{-1} at 0.585 A g^{-1}	197.6 Wh kg^{-1}	96 Wh kg^{-1}	This Work

References

[1] W. Weppner, R. A. Huggins, *J. Electrochem. Soc.* **1977**, *124*, 1569.

[2] Y. Fang, L. Xiao, J. Qian, Y. Cao, X. Ai, Y. Huang, H. Yang, *Adv. Energy Mater.* **2016**, *6*, 1502197.

[3] S. Li, Y. Dong, L. Xu, X. Xu, L. He, L. Mai, *Adv. Mater.* **2014**, *26*, 3545.

[4] Y. Zhang, H. Zhao, Y. Du, *J. Mater. Chem. A* **2016**, *4*, 7155.

[5] D. Wang, X. Bie, Q. Fu, D. Dixon, N. Bramnik, Y.-S. Hu, F. Fauth, Y. Wei, H. Ehrenberg, G. Chen, F. Du, *Nat. Commun.* **2017**, *8*, 15888.

[6] W. Ren, Z. Zheng, C. Xu, C. Niu, Q. Wei, Q. An, K. Zhao, M. Yan, M. Qin, L. Mai, *Nano Energy* **2016**, *25*, 145.